June 2020

Transcriptome Studies on the Toxicity of Silica Nanoparticles

Shih-Yi Hsu
University of South Florida

Transcriptome Studies on the Toxicity of Silica Nanoparticles

by

Shih-Yi Hsu

A thesis submitted in partial fulfillment
of the requirements for the degree of
Master of Science in Pharmaceutical Nanotechnology
Taneja College of Pharmacy
University of South Florida

Major Professor: Feng Cheng, Ph.D.
Vijaykumar Sutariya, M.Pharm., Ph.D., R.Ph.
Alya Limayem, Ph.D.
Sheeba Varghese Gupta, M.Pharm., Ph.D.

Date of Approval:
June 11, 2020

Keywords: nanotoxicities, bioinformatics, gene expression, pathway, genomic database, cell lines

Acknowledgment

Dr. Feng Cheng always gives me directions when I am confused with the progression of this project. I learn so many useful tips from Dr. Daniel Denmark. I also have many thanks to Dr. Limayem, Dr. Sutariya, and Dr. Gupta for being my committee members, to my family for their encouragement to me, as well as to people behind the scene. It is so wonderful to do research in such a supportive environment.

Table of Content

List of Tables

List of Figures

Abstract

Nanotechnology enables more precise harmony in health condition via reducing the dosage amount, improving the delivery of hydrophobic drugs, more specific targeting to the cancerous sites, and so on. Nevertheless, issues regarding the toxicity of nanotechnology have begun to call for attention several decades later after the innovation of nanotechnology. Tools about risk management of nanotechnology have been developed, but recently not much evidence recognizes the toxicity of nanoparticles (NPs) except for some animal studies, which demonstrated organ damage after the exposure to NPs. Toxicogenomic approach refers to the method utilizing gene expression to evaluate the chemical toxicity. Databases as Gene Expression Omnibus and Database for Annotation, Visualization, and Integrated Discovery are useful platform to provide information about genomic and genetic pathway. After comparing groups at 4 hours and 24 hours, our study reveals the toxicity of silicon dioxide (SiO_2) NPs to human aortic endothelial cells (HAECs) is affected by their morphology, and via regulation of different amounts of genes. Cytotoxicity is also related to materials as SiO_2 and poly-amido-amine. More analyses with SiO_2 NPs cultured with mouse macrophages and lung cancer cells, A549 cells, indicates the size as the attribute of silica nanotoxicity. Smaller SiO_2 particles appear to be more toxic in medium concentration. Among all these three cells (HAECs, mouse macrophages, and A549 cells), tumor necrosis factor (TNF) signaling pathway is the most highly up-regulated pathway. Therefore, the expression of TNF signaling pathway highlights the

sub cellular mechanism of toxicity resulted from silica NPs regardless of the morphology or the size of the particles, and the cell types.

Chapter 1: Introduction for toxicity of nanoparticle and toxicogenomics

1.1 Nanoparticles

The concept of 'nano' was developed more than half a century ago. Nanoparticles (NPs) demonstrate new physicochemical properties compared to their bulk materials. A nanometer is one billionth of a meter and is a useful unit of measure in many fields, such as diagnostic devices and therapeutic drugs in the medical field (Bhushan, B, 2017.; Kumar et al, 2013; Jain, K. K. 2017).

Not only does nanotechnology provide an alternative way to enhance drug delivery, the novel traits of NPs also provide useful ways as treatments (Patra et al., 2018). By applying NPs in drug delivery, the bioavailability of hydrophobic compounds is possible to be improved, and more precise delivery to diseased sites is able to be achieved with active targeting or stimulus related targeting. An innovative scope at the molecular level is built with nanomedicine in both diagnostic and therapeutic field (Kim, Rutka, & Chan, 2010). Currently, FDA has approved several drugs with nanotechnology such as PEGylations or liposomes (Bobo, Robinson, Islam, Thurecht, & Corrie, 2016). The pegylated products have longer circulation time and the drugs delivered by liposomes appear to have less toxicity (Alconcel, Baas, & Maynard, 2011; James et al., 1994). Due to the advantage of surface area to volume ratio, less dosage is required for the same therapeutic effects as nanocrystals (Jens-Uwe, 2008). The superparamagnetic character of iron oxide NPs is applied in diagnostic imaging tool (Bashir, Bhatti, Marin, & Nelson, 2015). A number of NPs have been explored and

investigated, so a future with less detrimental effects on healthy tissues while treating diseases will come.

1.2 Silica nanoparticles

The oxidized form of silicon, silica or silica dioxide (SiO_2), is the most abundant compound on earth. Several strengths of using silica nanoparticles (SNPs) are their low cost, convenience of scale-up, ability to be modified with surface groups, and their biocompatibility (Nafisi & Maibach, 2015). Fumed or pyrogenic silica has been used in cosmetics as solvable powder to prevent pigments from aggregation. It also soothes greasy skin and provides ultraviolet (UV) protection. SNPs also enhance the penetration of drugs into the dermis layer of the skin (Nafisi & Maibach, 2015). Moreover, they are used as additive agents in powder to prevent mass formation in food industry (Athinarayanan, Periasamy, Alsaif, Al-Warthan, & Alshatwi, 2014).

One method to make SNPs was using lysine as catalyst. Hydrolysis and water separation were involved in the process (Pirutchada et al., 2019). With adding surfactant as templates, porous SNPs were created (Patil, Verma, Patil, Naik, & Narkhede, 2019).

Mesoporous silica nanoparticles (MSNPs) were designed for cancer therapy because they were capable of loading drugs in the tunable pores and being delivered to the tumor sites. Adding organic part to the mesoporous silica platform improved their degradation (Guimaraes, Rodrigues, Moreira, & Correia, 2020). For example, loaded with 5-fluorouracil and NAD(P)H:quinone oxidoreductase 1 inhibitor, MSNPs coated with lipid bilayers reduced head and neck squamous cell carcinoma volume in mice model in addition to increasing cancer cell death (Chen et al., 2019). MSNPs loaded

with aceclofenac were demonstrated in vitro with the increasing half-life of aceclofenac (Patil et al., 2019). The delivery route of the drug might also be changed by MSNPs, such as oral insulin (Juère, Caillard, Marko, Del Favero, & Kleitz, 2020). Beside the advantage of carrying drugs with the pores, SNPs were easy to be manipulated with the surface morphology. By modifying the MSNPs with aptamer, Sgc8, doxorubicin was more selectively delivered to leukemia cells (Yang et al., 2019). With modification of the surface molecular group, MSNPs could release the loading drugs in acidic environment, or when they were stimulated by UV light at 365 nm wave length (Wang, Wang, Wang, Jiang, & Fu, 2019). Another research showed 12 nm SNPs resulted in the death of astrocytoma U87 cells, one kind of human brain tumor cells, when the concentration is above 25 μg/ml (Lai et al, 2010). Besides, in micro-electromechanical systems, SiO_2 film is a common part of cantilever fabrication (Bhatt & Chandra, 2007). When SNPs were doped with quantum dots and were further conjugated with antibodies, they could be used as fluorescent dye to visualize leukemia cells (Bottini et al., 2007). A better image quality derived when SNPs were doped with dyes and contained a gold core (Galanzha et al., 2017). Together, these evidences revealed the potential popularity of SNPs in the drug delivery and the diagnosis, although a gap between efficacy and safety may need to be overcome.

1.3 Toxicity of nanoparticles

In addition to the low delivery rate of NPs to tumors (Wilhelm et al, 2016), another hurdle is some evidence with toxicity in animal studies and in vitro studies, thus the term, nanotoxicity (Donaldson et al, 2004; Arora et al, 2011). The nanotoxicity describes the debilitating effects of nanoparticles on living systems as well as ecological

systems (Aggarwal et al, 2009). Human bodies are exposed to NPs through ocular, inhalational, dermal contact, oral and other numerous routes (Oberdörster et al, 2005).

Knowledge of adverse effects about NPs to vascular endothelial cells is crucial, while intravenous drug delivery is an effective way to treat systemic diseases or invasively diagnostic devices are adopted to detect blood components. Iron oxide NPs as imaging NPs induced inflammation response and oxidative stress to human aortic endothelial cells and umbilical endothelial cells as well as pulmonary fibrosis in animal model, despite no obvious toxicity in clinic for iron oxide NPs (Li et al. 2014, Zhu et al. 2010, 2011). In addition, CdTe is found to have dose-dependent cytotoxicity in human umbilical vein endothelial cells (Yan et al, 2011). Hemolytic toxicity of human red blood cells is found with larger size of modified or unmodified graphene oxide above 300 nm (Kiew et al, 2016; Liao et al, 2011). TiO_2 nanobelts (TiO_2-NB) are considered more toxic to THP-1 cells than multi-walled carbon nanotubes since evidence shows TiO_2-NB regulates gene pathways with inflammation, apoptosis and cell cycle arrest (Tilton et al, 2013). The shape of SiO_2 NPs as well as functional groups of poly(amido amine) (PAMAM) dendrimers have different levels of toxicity on human aortic endothelial cells. Spherical shape SiO_2 NPs are toxic at lower concentration than worm shape SiO_2. Carboxyl ended dendrimers seem to have less toxic effect than amine ended dendrimers (Moos et al, 2013).

1.4 Toxicogenomics

As early as in 1980s, scientists began to investigate the relationship between genes and toxicity. The niridazol, an agent against schistosomiasis, was researched for the relationship between its neurotoxicity and the Ah locus of mice (Blumer, Simpson,

Lucas, & Webster, 1980). Stemmed from the human genome project, plates coated with genetic materials as DNA arrays were being used to test the chemical toxicity, an approach named as a toxicogenomic model. Advocated by Lovett (2000), if this approach could overcome the puzzles between untested chemicals and actual outcomes such as real illness, toxicogenomic models might save the cost of experimental animals and detect chronic diseases as early as possible (Lovett, 2000).

Paved with this concept, big genomic data used to predict liver injury such as fibrotic and necrotic pathology with drug dosage in humans and mice was developed in the following years (Kohonen et al., 2017). In addition, it is possible to track the molecular pathways related with hepatitis B virus (HBV) in hepatocellular carcinoma (HCC). With the amount of 113 overlapping genes derived from two datasets, AMPK signaling pathway and responses to cadmium ions were likely to be involved in HBV related HCC (Li et al., 2020).

Toxicogenomic models can also be applied to assess nanotoxicities. Several databases were built despite scarce research in nanotoxicities. The NanoSolveIT project is an example, aimed to integrate these databases to provide a platform to predict adverse effects of nanomaterials based on their infrastructure, gene expression data, and various endpoints (Afantitis et al., 2020).

Through studying genomic expression of human cell lines after exposure to NPs, more understanding in the mechanism of toxicity caused by NPs is able to be revealed (Moos et al., 2013). In this project, we analyzed public transcriptome data on the toxicity of two drug delivery nanoplatforms for primary human aortic endothelial cells, as well as the toxicity of silica NPs on mice macrophages and lung cancer cells. The identified

genes and gene pathways may assist the risk management of these nanoplatforms. More specification of the affected genes owns the potential to assist the pharmaceutical industry in designing dosage and morphology of coming nano-components.

Chapter 2: Silica nanoparticle effects on human heart epithelial cell

2.1 Introduction

In this chapter, the transcriptional responses of primary HAECs to SNPs and PAMAM dendrimers were identified. We tried to see the gene changes of endothelial cells caused by these drug delivery nanoplatforms.

2.2 Methods and data set

The study was based on a National Center for Biotechnology Information's (NCBI) Gene Expression Omnibus (GEO) data set, GSE35142. In this data set, the effects on gene expression of HAECs by two different shapes of SNPs (sphere and worm) and carboxyl (COOH) PAMAM group and the amine (NH_2) PAMAM were investigated. The chemical structure of PAMAM was shown in Figure 1.

2.2.1 Gene Expression Omnibus database

Gene expression data was analyzed with the NCBI's GEO database (Edgar & Barrett, 2006). After searching with the keyword as "human aortic endothelial cells, silicon dioxide," further information was retrieved with clicking the "Analyze with GEO2R" tab (Figure 2). The website address was as follows: https://www.ncbi.nlm.nih.gov/geo/query/acc.cgi?acc=GSE35142.

2.2.2 Define groups

The SiO_2 and PAMAM groups were defined in NCBI GEO2R analyzer. Groups of the same material either SiO_2 or the dendrimer were compared between different time period as 4 hr and 24 hr. Groups with various materials modified differently were also

compared within the same time period, 4 hr and 24 hr respectively. For example, the group name was entered as "SiO_2 worm 4hr" after clicking the tab "define groups" and then select the following items with "200nm SiO_2 worm 4hr incubation 100 μg/ml." Next, another group named as "SiO_2 sphere 4hr" was created and filled with "200nm SiO_2 spheres 4hr incubation 73.38 μg/ml."

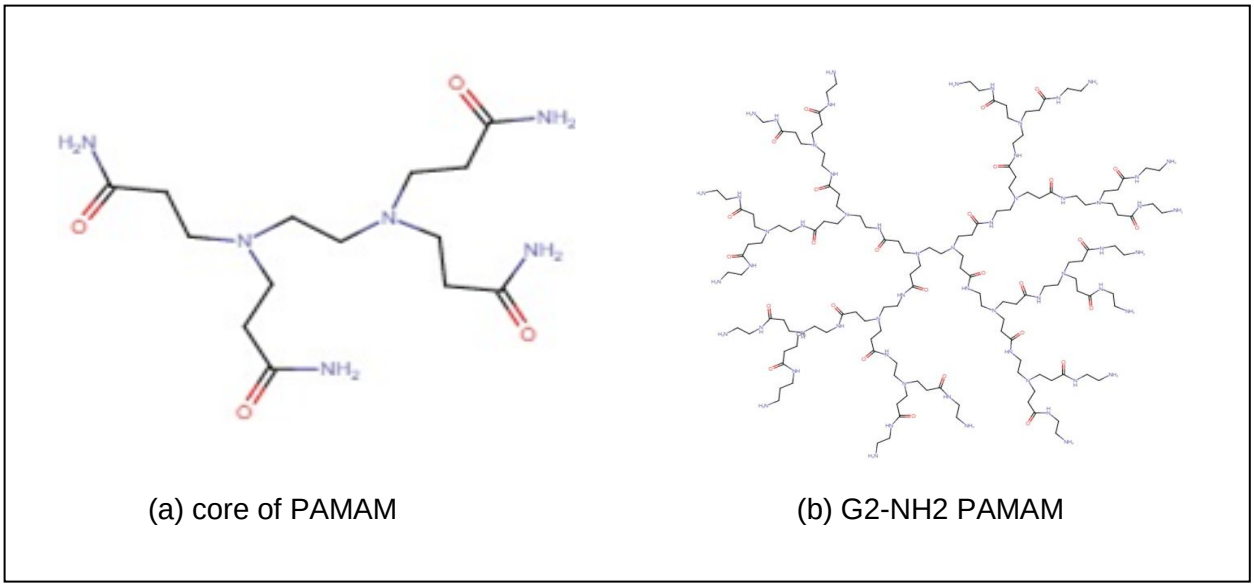

Figure 1. Chemical structure of PAMAM

Note. (a) The core of PAMAM was similar to ethane in the central with hydrogen atoms replaced by tertiary amine nitrogen atoms. The surface layers were four primary amide groups. In other words, ethylene diamine was used as a core initiator. (b) Dendrimers were synthesized with divergent or convergent process. The nitrogen in the amide groups acted as nitrogen in ethylene diamine and this forms one generation. Once the amide group was replaced by carboxyl group, this forms a half generation.

2.2.3 Refine the results of expressed gene

During this process, the actions were to hit the "TOP250" tab and click the "Save all results" link to open a new window. The data of gene lists was saved as text files (*.txt) after the processing is done. For statistical significance, the collected gene lists were organized by eliminating data with adjusted p value over 0.05. The up and down

regulated genes were further adjusted in accordance with log (Fold Change), which was labeled as log FC, more or less than 1 with Microsoft Excel software. The value of fold change (FC) as 1.25 was also considered.

Figure 2. Icon of the GEO database
Note. The icon was from the websites of Gene Expression Omnibus. In the figure, the tab for analyzing at the bottom of the website page was shown below.

2.2.4 Generation of genetic pathways

The refined gene list was entered into the Database for Annotation, Visualization and Integrated Discovery (DAVID) (https://david.ncifcrf.gov) to generate Kyoto Encyclopedia of Genes and Genomes (KEGG) pathways (Dennis et al., 2003). The gene list was analyzed through functional annotation domain and under official gene symbol. *Homo sapiens* was designated as our species. The species was changed in mouse model.

2.2.5 Computer hardware system and settings

The databases were run by Dell OptiPlex 3060 desktop computer core and Mac. The operating systems include Windows 10 developed by Microsoft Corporation and the search engine is Google Chrome.

2.3 Results

2.3.1 Differentially expressed genes

Four materials, including worm shaped (100 μg/ml) and spherical shaped (73.38 μg/ml) SiO_2 NPs, sizing around 200nm, COOH-PAMAM and NH_2-PAMAM dendrimer were analyzed. The gene expression level difference of each material between 4 hr and 24 hr were compared. The survivals of HAECs cells cultured with these 4 materials were also obtained.

In toxicogenomics, the number of differentially expressed genes was a good measurement to evaluate the effects of treatment on a biological system. In our studies, we found there was a strong association between the number of differentially expressed genes and cell viability. In the HAECs data set, cell survival and transcriptome profiles of the endothelial cells were observed after 4 hours and 24 hours with conditions when cells were transfected with NPs of various morphologies and compositions. For instance, the quantities of regulated genes by spherical SNPs were analyzed between 4 and 24 hours.

As shown in Table 1, after 24 hours, there was a 57% (from 100% to 43%) decline in cell population for cells treated with SiO_2 sphere shape NPs at a concentration of 100 μg/ml. Between 4 hours and 24 hours post-transfection, 4411 genes were found to be regulated at adjusted p-value < 0.05 and at least 1.25 fold

change. Transfection with worm formed SiO_2 NPs resulted in a 19% (decreasing from 100% to 81%) cell mortality rate and 368 differentially regulated genes after 24 hrs. Transfection with either the COOH-PAMAM nano construct or the NH_2-PAMAM nano construct resulted in no cell mortality. A total of 2 and 15 differentially expressed genes were found for NH_2-PAMAM and COOH-PAMAM material by comparing transcriptome of 4 hours with 24 hours.

Table 1. Association of gene number and cell survival

Nano_Construct	Concentration	Cell Survivor%	#Regulated genes (4hr vs 24hr)
SiO_2_Worm	100 µg/ml	81	368
SiO_2_Sphere	73 µg/ml	43	4426
G3.5-COOH_PAMAM	0.5 µM	103	15
G4-NH_2_PAMAM	0.5 µM	100	2

Note. The regulated gene number is composed of both up and down regulated genes. The gene number are values after comparing 24 hr group with 4 hr group of different nano constructs, and the results with blank gene identity are eliminated.

The linear relationship between the number of differentially expressed genes and the percentage of cell survival was shown in the Figure 3; there was a positive correlation between the cytotoxicity of the NPs and the number of differentially

expressed genes, of which a greater cell mortality rate was associated with a higher number of dysregulated genes. Since no cytotoxicity was observed with PAMAM groups, we defined a control group with all PAMAM materials. The control group was compared with worm and sphere shaped SNPs selected in one group.

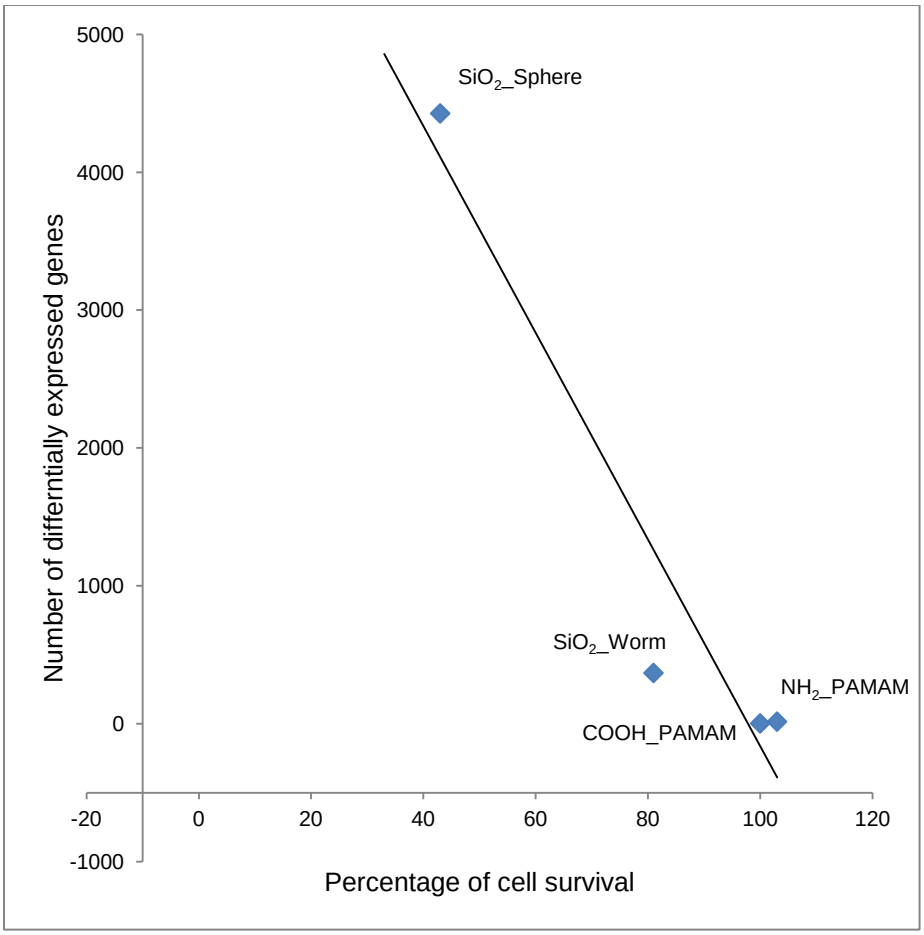

Figure 3. The association between the number of differentially expressed genes with cell survival

Note. The correlation was noted in the figure. Generally, the more the differential expressed genes were affected, the less survival chance the cells had. Spherical SNPs affected more genes than worm shaped SNPs, so the percentage of HAECs cultured with the spherical SNPs was less. Moreover, the figure showed SNPs were more toxic than PAMAM.

The levels of the differentially regulated genes as a result of comparing SNPs with PAMAM were demonstrated in Figure 4. More genes were up regulated by the

group of SNPs than the number of genes down regulated when SNPs was compared with PAMAM.

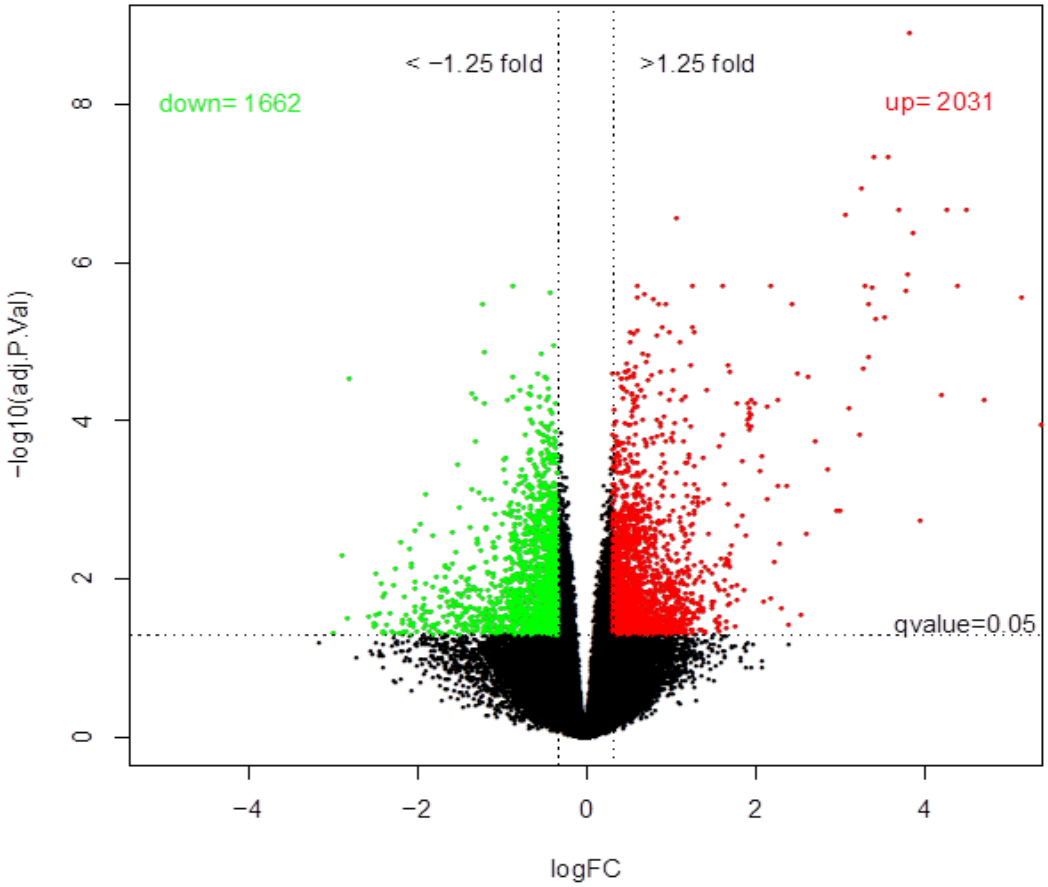

Figure 4. Gene regulated by silica nanoparticles

Note. The genes are compared by using PAMAM as the control group. The red spots indicated the up regulated genes, so do the green spots. There are 2031 up-regulated and 1662 down-regulated genes for silica material comparing with PAMAM.

2.3.2 Gene pathways and ontology analysis

The genetic pathways in Figure 5 were listed according to the level of fold change. Among these pathways, TNF signaling pathways were the most overly expressed one when comparing SNPs with PAMAM as described in the previous section. More details with the genes involved in the genetic pathways were given in Table 2.

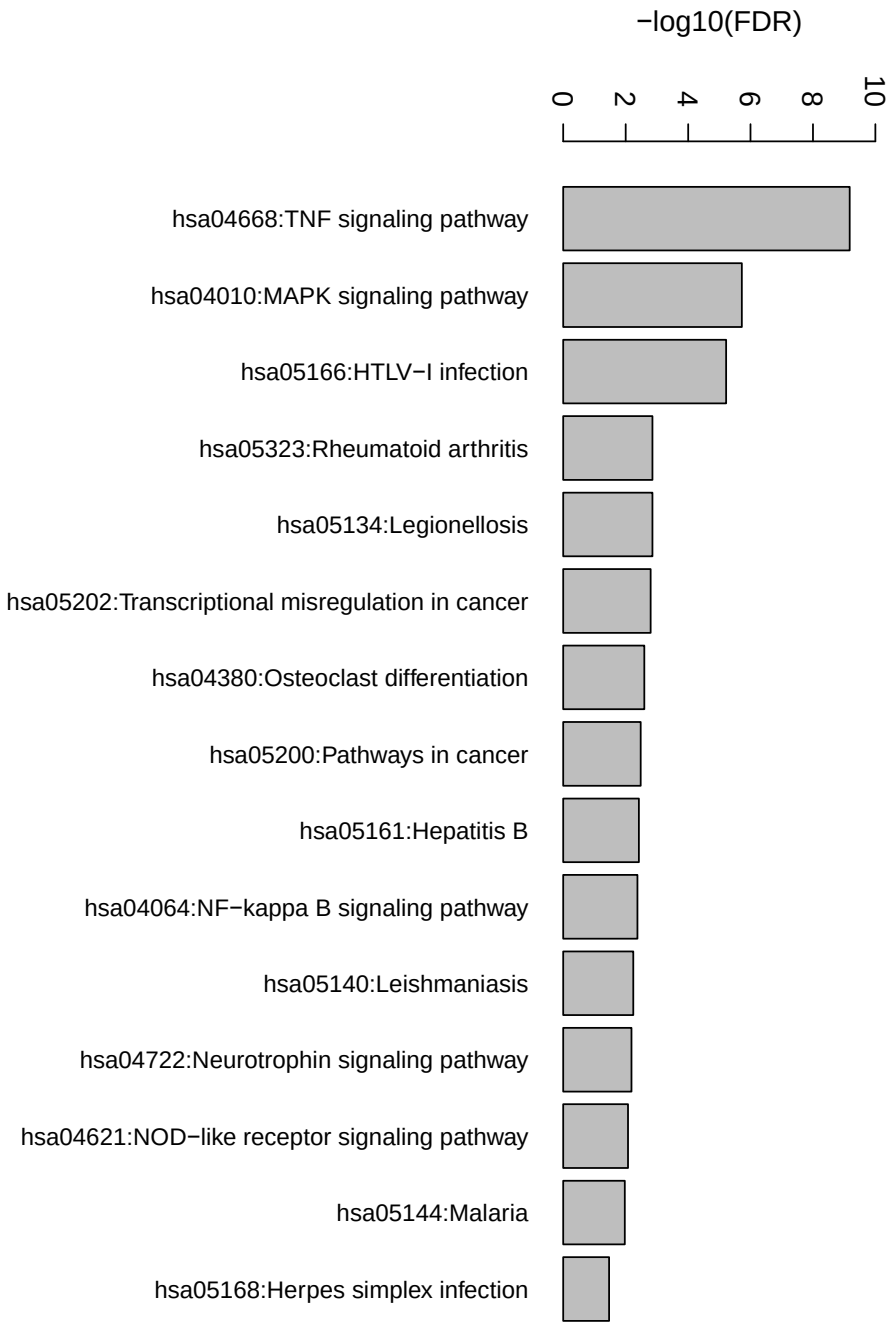

Figure 5. Enriched gene pathways in up-regulated genes

Note. TNF signaling pathway has the most statistical significance. These pathways are derived from the gene list by comparing silica NPs with PAMAM.

Table 2. Enriched Pathways in up-regulated genes in human sample

Term	Count	PValue	Genes	Fold Enrichment	FDR (%)
hsa04668:TNF signaling pathway	29	5.13E-11	TRAF1, CSF2, TNF, CCL2, PTGS2, CXCL3, CXCL2, NFKBIA, NFKB1, ATF2, VCAM1, LIF, FOS, CCL20, MAP3K8, BCL3, IL1B, ICAM1, SOCS3, MAP2K3, CREB1, MAPK11, CREB5, BIRC3, JUNB, RPS6KA5, JUN, TNFAIP3, SELE	4.27	6.68E-08
hsa04010:MAPK signaling pathway	40	1.46E-07	FGF5, TNF, DUSP10, NFKB1, HSPA1A, CACNB3, NFKB2, FGF12, ATF2, FOS, BDNF, RAC3, ELK4, MAP3K1, MAPT, SOS1, MAP3K8, DUSP16, RASGRP2, IL1B, IL1A, NFATC1, MAP2K5, LAMTOR3, MAP2K3, RELB, NR4A1, MAPK11, DDIT3, CDC25B, MAP4K3, RPS6KA5, DUSP5, RPS6KA6, DUSP2, DUSP1, RPS6KA2, JUN, GADD45B, MAP3K11	2.49	1.90E-04
hsa05166:HTLV-I infection	39	4.66E-07	CSF2, CRTC2, NRP1, TNF, CREM, ADCY6, NFKBIA, NFKB1, NFYB, ITGB2, NFKB2, CANX, ATF1, ATF2, VCAM1, FOS, ELK4, MAP3K1, NFATC2, TBPL1, NFATC1, FZD9, EGR1, ZFP36, ICAM1, KAT2B, EGR2, SLC25A6, CREB1, RELB, POLB, RB1, FZD5, DVL1, CDKN1A, ATF3, ETS1, JUN, WNT9A	2.42	6.06E-04

Note. Details of the genes involved in different pathways up regulated by SNPs. The gene abbreviations, the count of genes in each pathway, p-values, adjusted p-values (FDR), and the value of logarithmic function with pathway fold change (fold enrichment) were listed in the table.

Table 2. (Continued)

hsa05323:Rheumatoid arthritis	17	1.07E-04	ICAM1, CSF2, TNF, CCL2, TLR2, CXCL8, ACP5, ITGB2, ATP6V1B2, FOS, CCL20, JUN, ATP6V1E1, TEK, IL1B, IL1A, CD28	3.04	0.14
hsa05134:Legionellosis	13	1.08E-04	EEF1A1, TNF, CXCL3, CXCL2, TLR2, CXCL8, NFKBIA, EEF1G, IL1B, NFKB1, ITGB2, HSPA1A, NFKB2	3.79	0.14
hsa05202:Transcriptional misregulation in cancer	25	1.23E-04	CCNT2, TRAF1, BMI1, CEBPA, NFKBIZ, CSF2, RXRB, RXRA, MET, CXCL8, NFKB1, SIX4, DDIT3, ATF1, MLF1, CDKN1A, CDKN1B, TAF15, REL, ELK4, PER2, MDM2, RARA, JMJD1C, KLF3	2.36	0.16
hsa04380:Osteoclast differentiation	21	1.96E-04	TNF, FOSL2, SOCS3, CREB1, RELB, NFKBIA, ACP5, NFKB1, MAPK11, NFKB2, FOSB, STAT1, JUNB, CYLD, FOS, SQSTM1, JUN, IL1B, NFATC2, IL1A, NFATC1	2.52	0.26
hsa05200:Pathways in cancer	44	2.54E-04	TRAF1, FGF5, PTGS2, PGF, ADCY6, CXCL8, NFKBIA, KITLG, NFKB1, NFKB2, FGF12, ITGB1, GLI1, FOS, RAC3, SOS1, RASGRP2, RALB, NKX3-1, RARA, TRAF4, FZD9, CEBPA, RXRB, RXRA, MET, RB1, FZD5, STAT1, BIRC3, DAPK3, RALGDS, DVL1, CDKN1A, CDKN1B, PLCG1, GNAQ, ETS1, JUN, RASSF1, MDM2, LAMC2, GNAS, WNT9A	1.76	0.33

Table 2. (Continued)

hsa05161:Hepatitis B	22	2.90E-04	EGR3, TNF, EGR2, CREB1, DDB1, TLR2, CXCL8, NFKBIA, NFKB1, CREB5, RB1, STAT1, ATF2, STAT6, FOS, CDKN1A, CDKN1B, JUN, MAP3K1, TICAM1, NFATC2, NFATC1	2.39	0.38
hsa04064:NF-kappa B signaling pathway	16	3.23E-04	TRAF1, ICAM1, TNF, PTGS2, RELB, CXCL8, NFKBIA, UBE2I, NFKB1, NFKB2, BIRC3, VCAM1, PLCG1, TICAM1, IL1B, TNFAIP3	2.89	0.42
hsa05140:Leishmaniasis	14	4.39E-04	TNF, PTGS2, NFKBIB, TLR2, NFKBIA, NFKB1, ITGB2, MAPK11, STAT1, ITGB1, FOS, JUN, IL1B, IL1A	3.10	0.57
hsa04722:Neurotrophin signaling pathway	19	5.05E-04	IRAK2, NFKBIE, NFKBIB, NFKBIA, NFKB1, MAPK11, RPS6KA5, RPS6KA6, BDNF, PLCG1, RPS6KA2, JUN, MAP3K1, SOS1, GAB1, PSEN2, CAMK2D, RIPK2, MAP2K5	2.49	0.66
hsa04621:NOD-like receptor signaling pathway	12	6.46E-04	TNF, CCL2, NFKBIB, CXCL2, CXCL8, RIPK2, NFKBIA, IL1B, NFKB1, MAPK11, BIRC3, TNFAIP3	3.37	0.84
hsa05144:Malaria	11	8.27E-04	VCAM1, ICAM1, TNF, CD36, CCL2, MET, TLR2, CXCL8, IL1B, ITGB2, SELE	3.53	1.07
hsa05168:Herpes simplex infection	23	0.0026	TRAF1, HMGN1, GLTSCR2, TNF, CCL2, SOCS3, NFKBIB, TLR2, NFKBIA, NFKB1, HCFC2, CDC34, STAT1, FOS, TAF5L, GTF2I, GTF2IRD1, JUN, TICAM1, PER2, IL1B, EIF2AK3, TBPL1	1.98	3.40

Chapter 3: Silica nanoparticle effects on mouse macrophage

3.1 Introduction

In this chapter, the gene expression changes of RAW 264.7 mouse macrophage cells regulated by two different sizes of amorphous SNPs (10 nm and 500 nm) at three different doses were identified. These three doses were labeled as low, medium, and high concentration.

3.2 Data set

The study described in this chapter was based on a NCBI GEO data set, GSE13005. In this data set, the effects on gene expression of RAW 264.7 mouse macrophage cells by 10 nm silica at 5 (low), 20 (medium), or 50 (high) μg/ml for 2 hours, as well as 500 nm silica at 250 (low), 500 (medium), or 1000 (high) μg/ml, were investigated.

3.3 Results

3.3.1 Differentially expressed genes

The results of the differentially expressed genes with 10 nm and 500 nm SNPs were shown in Figure 6 and Figure 7 respectively. The colored spots, as green and red, represented the results with statistical significance of adjust p value (q value) less than 0.05 and the Fold Change more or less than 1.25. The results without statistically significance were shown as black spots. At high dosage, more than 300 genes were regulated by both 10 nm and 500 nm SNPs. On the contrary, 10 nm particles were able to cause more gene changes than 500 nm NPs at medium dosage (Figure 8).

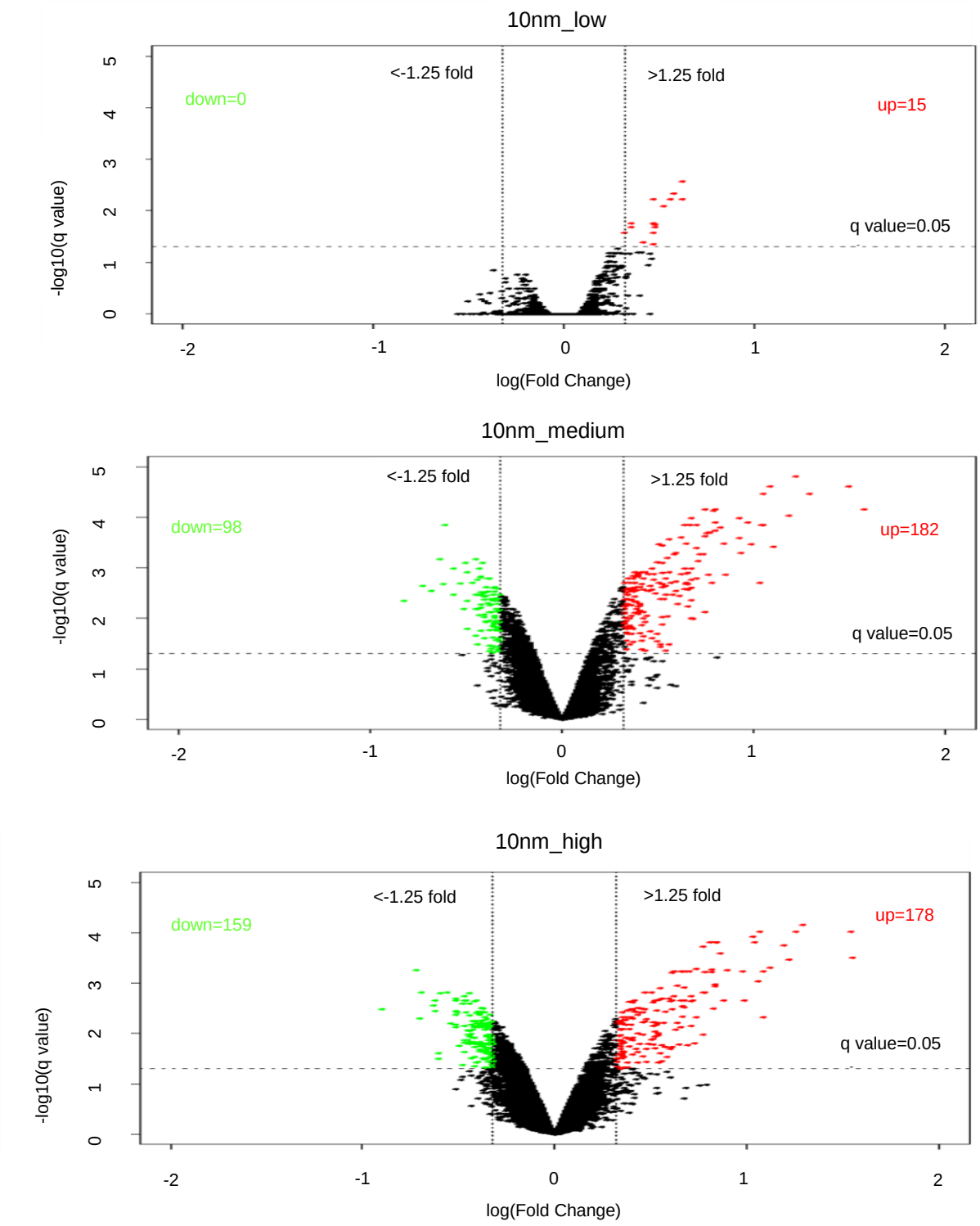

Figure 6. Regulated genes by 10nm SNPs at low, medium and high concentration

Note. More differentially expressed genes were noted when the concentration became higher. Nevertheless, most genes (182) were up regulated with the medium concentration. The q value here was defined as adjust p value.

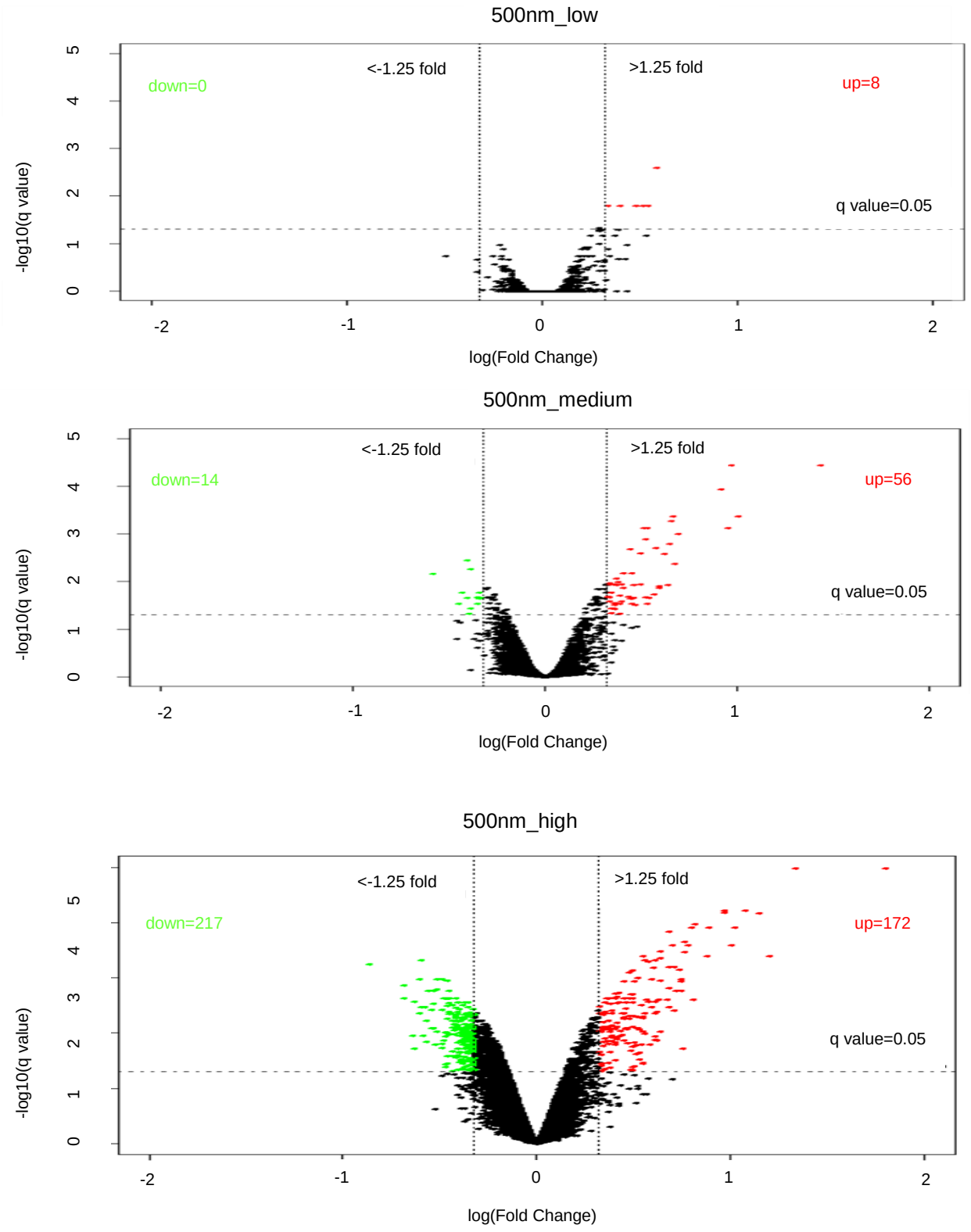

Figure 7. Regulated genes by 500nm SNPs at low, medium and high concentration
Note. Higher concentration was related to more differentially expressed genes.

3.3.2 Gene pathways and ontology analysis

Some enriched KEGG pathways with FDR value less than 0.05 were identified in up-regulated genes by NPs (Figure 8). Other than the medium concentration, 500 nm SNPs regulated more gene pathways than 10 nm SNPs at high concentration for 2 hours. TNF signaling pathway (mmu04668) was the top pathway for both materials. Other common gene pathways regulated by these two sized NPs included MAPK signaling pathway, HTLV-I infection, cytokine-cytokine receptor interactions and Chagas disease. There was no enriched gene pathway shown in genes down regulated by 10 nm or 500 nm SNPs.

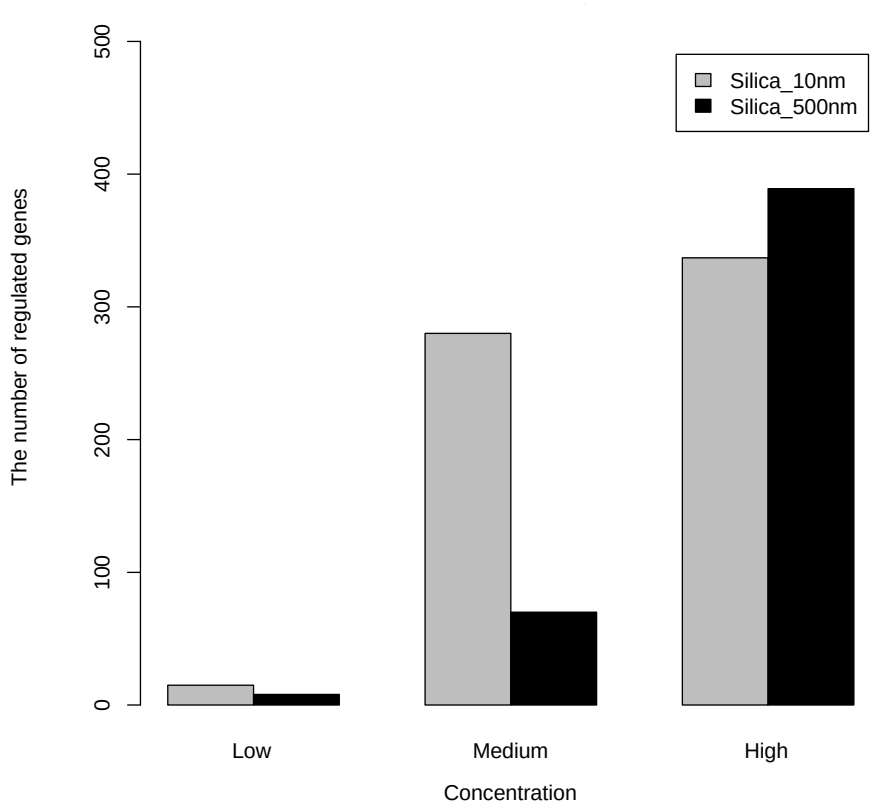

Figure 8. The number of regulated genes by different sizes SNPs at low, medium and high concentration

Note. 10 nm SNPs regulated more genes in medium concentration than 500 nm SNPs. More genes were affected when the concentration became higher.

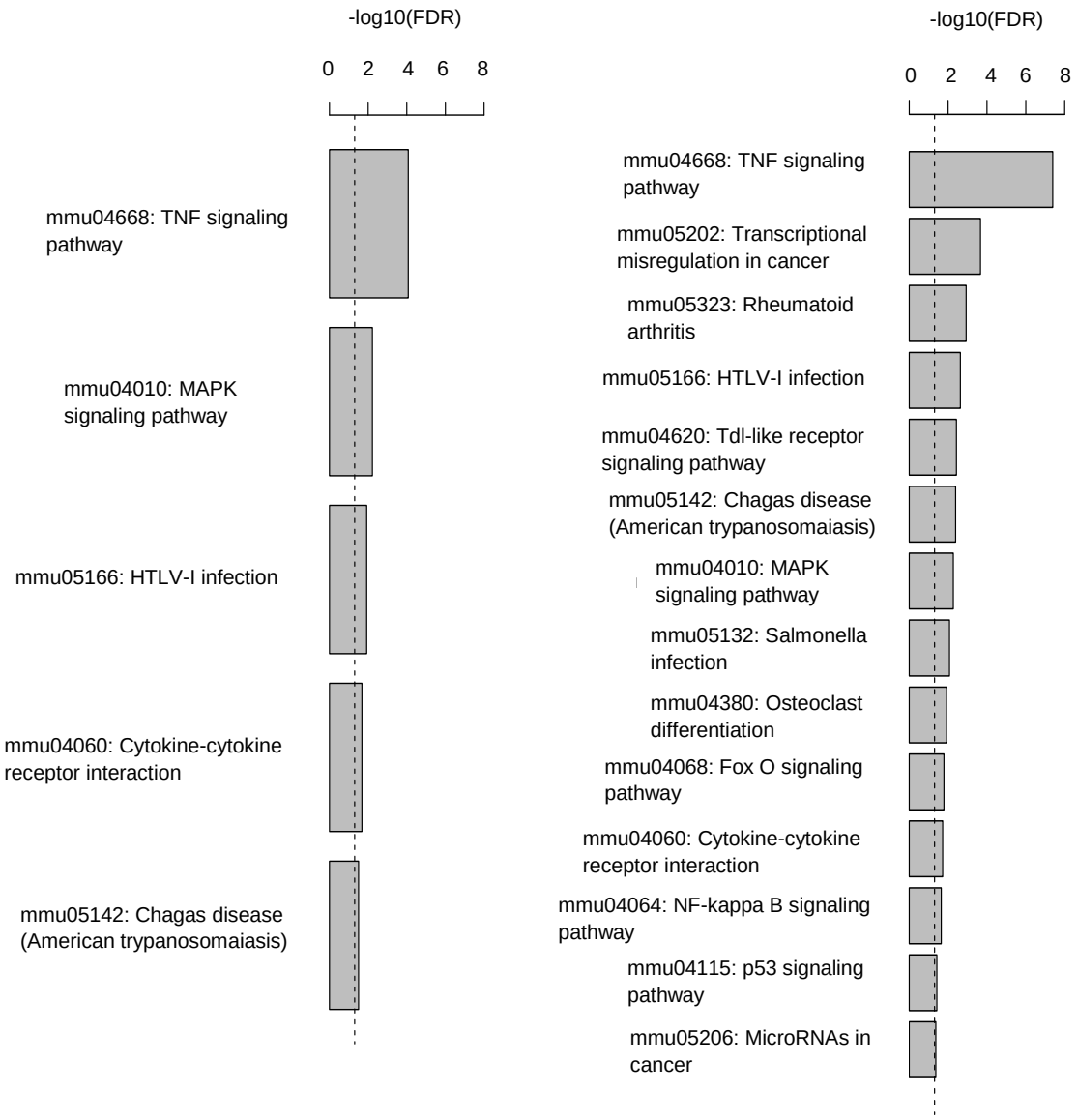

(a) 10nm nanoparticle at high concentration **(b) 500nm nanoparticle at high concentration**

Figure 9. Enriched gene pathways in up-regulated genes with both sized SNPs
Note. TNF signaling pathway was up-regulated in both 10 nm and 500 nm groups. Genetic pathways of low and medium concentration were not shown.

Chapter 4: Silica nanoparticle effects on A549 lung cancer cells

4.1 Introduction

In this chapter, the gene expression changes of A549 lung cell lines regulated by two different sizes of SNPs (9 nm and 18 nm of diameter) were identified.

4.2 Data set

The study was based on a NCBI GEO data set, GSE53700. In this data set, the effects on gene expression of A549 lung cancer cells by two different sizes of SNPs (9 nm and 18 nm of diameter) were investigated.

4.3 Results

4.3.1 Differentially expressed genes

In the group with 9 nm SNPs, 910 genes were up-regulated and 340 genes were down-regulated. On the other hand, no differentially expressed genes were found in the group with 18 nm SNPs (Figure 10). The genes that were expressed twice more were analyzed with fold change as 2 and log (Fold Change) as 1.

4.3.2 Gene pathways and ontology analysis

More than 20 KEGG pathways were found in A549 lung cancer cell lines after 3 hour exposure to 9 nm SNPs as shown in Figure 11. Among them, 18 KEGG pathways with Benjamini value less than 0.05 reached statistical significance. These pathways are TNF signaling pathway, pathways in cancer, rheumatoid arthritis, transcriptional regulation in cancer, cytokine-cytokine-receptor interaction, TGF-beta signaling pathway, hematopoietic cell lineage, MAPK signaling pathway, signaling pathways

regulating pluripotency of stem cells, proteoglycans in cancer, NF-kappa B signaling pathway, HTLV-I infection, amoebiasis, Fc epsilon RI signaling pathway, NOD-like receptor signaling pathway and so on. TNF signaling pathway again appears in the list as the most significant regulatory pathway of SNPs.

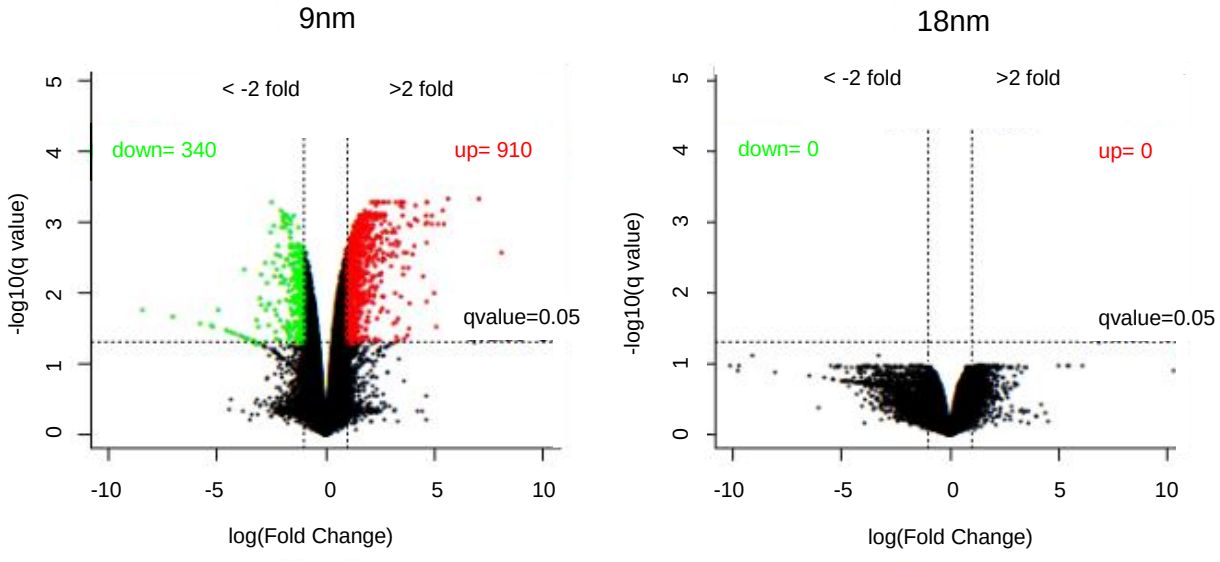

Figure 10. Regulated genes by different sizes SNPs in A549 cells

Note. More genes were regulated in 9 nm group than 18 nm group. No genes were found regulated in the 18 nm group. The q value here was equal to adjust p value.

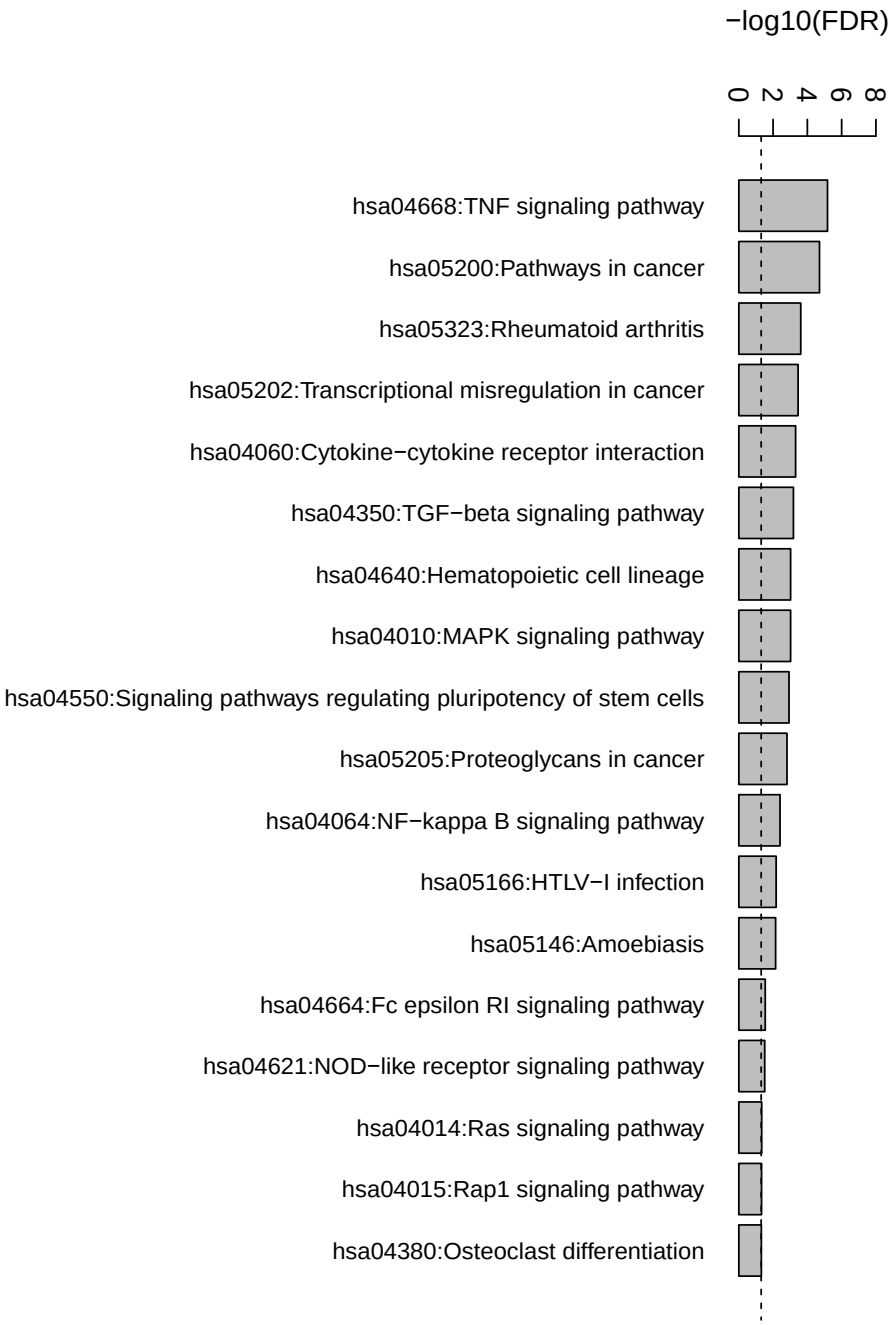

Figure 11. Enriched gene pathways in up-regulated genes in A549 cells

Note. TNF signaling pathway was up-regulated the most by 9 nm SNPs with A549 cells as noted in the figure. No down regulated gene pathways were found.

Chapter 5: Possible pathways and mechanism of toxicity caused by silica nanoparticles

TNF signaling pathway is a crucial way in regulating cell survival and death (Figure 11). Tumor necrosis factor (TNF) is a term coined by researcher as a serum factor that results in tumor regression. Shrinkage of tumor size and hemorrhagic necrosis are found after injection of lipopolysaccharide and BCG in a mouse model (Old, 1985).

Two pathways with TNF-R1 and TNF R2 receptors are found currently, and there are two molecules, TNF alpha and TNF beta. More studies are done on TNF-R1 and TNA alpha. Multiprotein signaling complex is formed during the process TNF signaling pathway. A variety of human diseases are related to this pathway, and it is the target of drug in immune disease such as rheumatoid arthritis. After extracellular domain of TNF-R1 binds to TNF, a homotrimer of 157 amino acid subunits, TNF-R1's intracellular domain (ICD) is revealed by separating from silencer of death domains (SODD) (Chen & Goeddel, 2002). ICD then binds to adaptor protein, TNF receptor-associated death domain (TRADD), and recruits additional adaptor proteins: TNF-R-associated factor 2 (TRAF2), receptor-interacting protein (RIP), and Fas-associated death domain (FADD). The recruiting of Caspase-8 following FADD initiates a protease cascade for apoptosis. Other parts of the TNF and TNF-R1 signaling pathway involve various activations of enzymes result in anti-apoptosis or NFκB activation (Chen & Goeddel, 2002). In endothelial cells, TNF induces cell death and a procoagulation state. However, studies

show TNF-R2 in favor of cell apoptosis rather than TNF-R1 pathway, which reduces cell death (Nawroth & Stern, 1987; Okada et al, 2001).

TNF alpha is a soluble polypeptide factor, or a cytokine, that serves as crosstalk between cells. It is composed of 20 proteins from the 18 genes located on the position of chromosome 7p21. It is produced by many cells including active B and T cells, mast cells, macrophages and monocytes, etcetera (Weinberg & Buchholz, 2006). The major source of TNF alpha is from activated macrophages. In addition to effects on antiviral activities, cellular metabolism, growth regulation of cells, coagulation processes, and insulin response, TNF alpha can trigger series of inflammatory processes, favoring antimicrobial response with inflammatory CD4 T cells (Th1) than atopic or allergic response with helper CD4 T cells (Th2). In endothelial cells, it aggravates vascular leakage and recruits lymphocytes. It also activates macrophages, increasing nitric oxide production (Weinberg & Buchholz, 2006). Therefore, some drugs focus on TNF alpha as the target to treat the disease. Other than TNF-alpha, which is mainly related to chronic systemic inflammatory response, TNF-beta is secreted by T cells and enhances phagocytic function of neutrophil and macrophages as well as cytotoxicity on tumor cells (Weinberg & Buchholz, 2006).

Several studies use TNF alpha to evaluate the effect like oxidative stress by SNPs on cells. Silica nanoparticles around 10 nm were found to induce TNF alpha in 3D alveolar model as well as interleukin-1 in a concentration dependent manner (Skuland et al., 2020). Moreover, spherical SNPs between 10 and 50 nm induced TNF alpha mRNA expression in human lung fibroblast cells by quantitative RT-PCR (Athinarayanan, Periasamy, Alsaif, Al-Warthan, & Alshatwi, 2014). Another study with

human lung fibroblast cells showed silica in nano form had more TNF alpha expression than their micro form with western blotting, indicating more toxicity in nano form (Ahmad, Khan, Patil, & Chauhan, 2012). This result was similar to the result with 3D alveolar model. TNF alpha was not specific to SNPs. Different nanomaterials could induce TNF alpha rather than SNPs in human monocytes (Ainslie et al., 2009), and SNPs induced other pathways, too. One major component of silymarin, silibinin, was found to reduce the TNF alpha expression due to SNPs as wells as mitogen-activated protein kinase and thioredoxin-interacting protein (Lim et al., 2020). These evidences are consistent with our study that silica nanoparticles regulate cell toxicity through TNF signaling pathway. Moreover, common genes are found in human and mouse model of TNF signaling pathway as shown in Table 3.

Table 3. TNF Pathways with up-regulated genes in human and mouse cells

Term	Count	PValue	Genes	Fold Enrichment	FDR (%)
hsa04668:TNF signaling pathway	29	5.13E-11	TRAF1, CSF2, **TNF, CCL2, PTGS2**, CXCL3, **CXCL2**, NFKBIA, NFKB1, ATF2, VCAM1, **LIF, FOS**, CCL20, MAP3K8, BCL3, IL1B, ICAM1, SOCS3, MAP2K3, CREB1, MAPK11, CREB5, BIRC3, **JUNB**, RPS6KA5, **JUN**, TNFAIP3, SELE	4.27	6.68E-08
mmu04668:TNF signaling pathway	11	7.58E-09	**LIF,** CFLAR, **FOS**, **CCL2**, **TNF**, **PTGS2**, **JUN**, CSF1, **CXCL2,** EDN1, **JUNB**	12.94	8.86E-08

Note. Different genes are regulated in human versus mouse model.

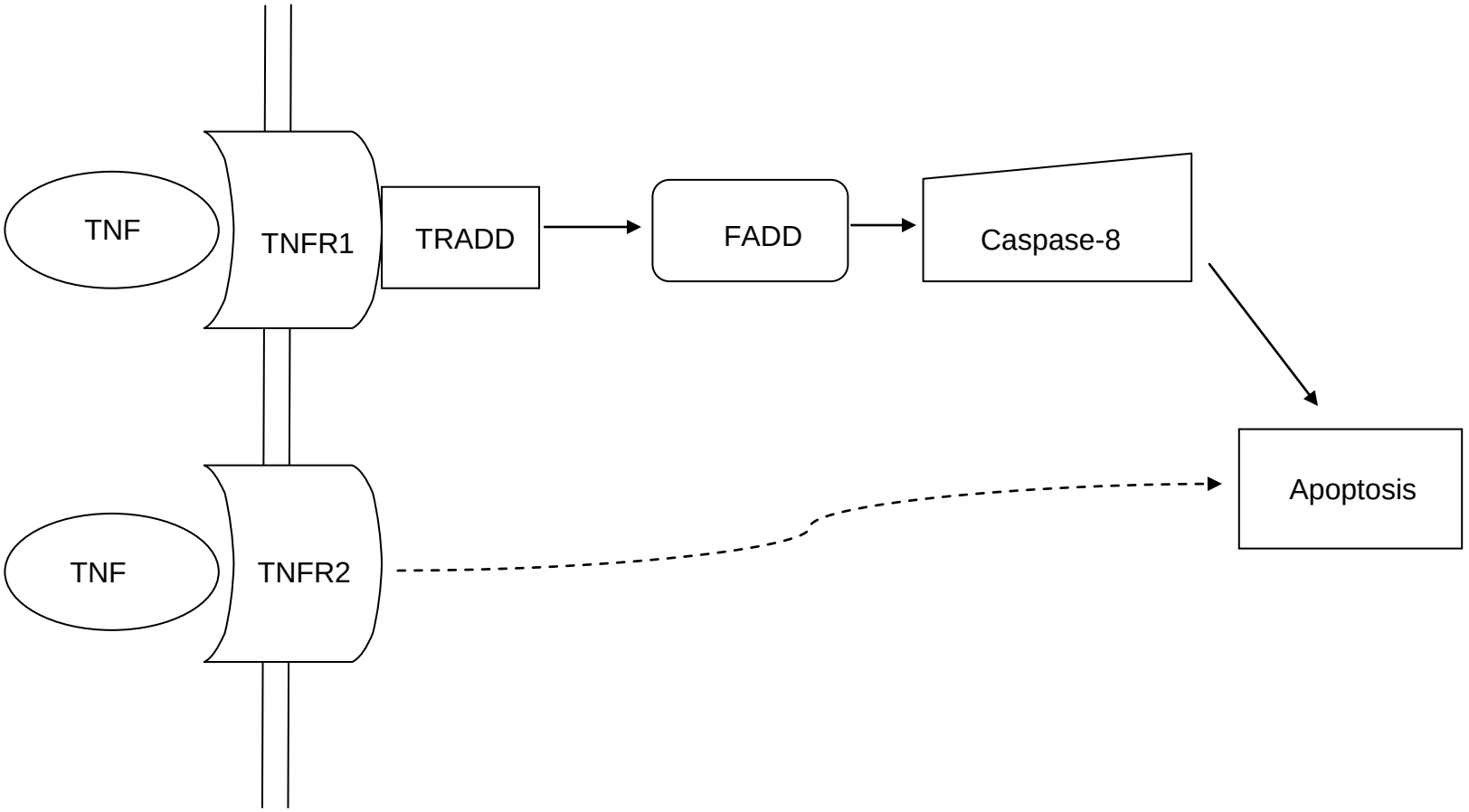

Figure 12. TNF signaling pathway

Note. TNF signaling pathway as membranous receptor (TNFR1 or TNFR2) interacts with TNF signal. A series of reactions inside the cell are demonstrated, leading to cell death. This is a concise figure. More proteins and chemical compounds can be involved in this pathway.

Chapter 6: Conclusion

In summary, gene number is related to cell survival in human aortic endothelial cells cultured with different materials, shapes, and functional group. Small sized silica nanoparticles are more toxic in medium concentration in mouse macrophages and lung cancer cells. Tumor necrosis factor signaling pathway is the main pathway involved in the toxicity mechanism of silica nanoparticles no matter what the size, the shape of the silica NPs is, or no matter what kind of the cells is.

References

Afantitis, A., Melagraki, G., Isigonis, P., Tsoumanis, A., Varsou, D. D., Valsami-Jones, E., . . . Lynch, I. (2020). NanoSolveIT Project: Driving nanoinformatics research to develop innovative and integrated tools for in silico nanosafety assessment. Comput Struct Biotechnol J, 18, 583-602. doi:10.1016/j.csbj.2020.02.023

Aggarwal, P., Hall, J. B., Mcleland, C. B., Dobrovolskaia, M. A., & Mcneil, S. E. (2009). Nanoparticle interaction with plasma proteins as it relates to particle biodistribution, biocompatibility and therapeutic efficacy. Advanced Drug Delivery Reviews, 61(6), 428–437. doi: 10.1016/j.addr.2009.03.009

Ahmad, I., Khan, M. I., Patil, G., & Chauhan, L. K. (2012). Evaluation of cytotoxic, genotoxic and inflammatory responses of micro- and nano-particles of granite on human lung fibroblast cell IMR-90. Toxicol Lett, 208(3), 300-307. doi:10.1016/j.toxlet.2011.11.004

Ainslie, K. M., Tao, S. L., Popat, K. C., Daniels, H., Hardev, V., Grimes, C. A., & Desai, T. A. (2009). In vitro inflammatory response of nanostructured titania, silicon oxide, and polycaprolactone. J Biomed Mater Res A, 91(3), 647-655. doi:10.1002/jbm.a.32262

Alconcel, S. S., Baas, A., & Maynard, H. (2011). FDA-approved poly(ethylene glycol)-protein conjugate drugs, 1442.

Arora, S., J. M. Rajwade, and K. M. Paknikar.(2012). Nanotoxicology and in vitro studies: The need of the hour. Toxicology and Applied Pharmacology 258(2):151–165. doi: 10.1016/j.taap.2011.11.010

Athinarayanan, J., Periasamy, V. S., Alsaif, M. A., Al-Warthan, A. A., & Alshatwi, A. A. (2014). Presence of nanosilica (E551) in commercial food products: TNF-mediated oxidative stress and altered cell cycle progression in human lung fibroblast cells. Cell Biol Toxicol, 30(2), 89-100. doi:10.1007/s10565-014-9271-8

Bashir, M. R., Bhatti, L., Marin, D., & Nelson, R. C. (2015). Emerging applications for ferumoxytol as a contrast agent in MRI, 884.

Bhatt, V., & Chandra, S. (2007). Silicon dioxide films by RF sputtering for microelectronic and MEMS applications. Journal of Micromechanics and Microengineering, 17(5), 1066–1077. doi: 10.1088/0960-1317/17/5/029

Bhushan, B. (2017). Springer handbook of nanotechnology. 3rd. Pages 1-9 [electronic resource]. Springer. Retrieved from http://search.ebscohost.com/login.aspx?direct=true&db=cat00847a&AN=usflc.02 2439300&site=eds-live

Blumer, J. L., Simpson, J. M., Lucas, S. V., & Webster, L. T., Jr. (1980). Toxicogenetics of niridazole in inbred mice. J Pharmacol Exp Ther, 212(3), 509-513.

Bobo, D., Robinson, K. J., Islam, J., Thurecht, K. J., & Corrie, S. R. (2016). Nanoparticle-Based Medicines: A Review of FDA-Approved Materials and Clinical Trials to Date. Pharm Res, 33(10), 2373-2387. doi:10.1007/s11095-016-1958-5

Bottini, M., D'Annibale, F., Magrini, A., Cerignoli, F., Arimura, Y., Dawson, M. I., . . . Mustelin, T. (2007). Quantum dot-doped silica nanoparticles as probes for targeting of T-lymphocytes. Int J Nanomedicine, 2(2), 227-233.

Chen, G. & Goeddel, D.V. (2002). TNF-R1 Signaling: A Beautiful Pathway. Science, 296(5573), 1634–1635. doi: 10.1126/science.1071924

Gilmore, T. D. (2006). Introduction to NF-κB: players, pathways, perspectives. Oncogene, 25(51), 6680–6684. doi: 10.1038/sj.onc.1209954

Chen, J., Zhang, S., Zhang, S., Gao, S., Wang, J., Lei, D., . . . Sun, H. (2019). Mesoporous Silica Nanoparticle–Based Combination of NQO1 Inhibitor and 5-Fluorouracil for Potent Antitumor Effect Against Head and Neck Squamous Cell Carcinoma (HNSCC). Nanoscale Research Letters, 14(1), 1-12. doi:10.1186/s11671-019-3224-3

Dennis, G. Jr., Sherman, B. T., Hosack, D. A., Tang, J., Gao, W., Lane, H. C., & Lempicki, R. A. (2003) DAVID: Database for Annotation, Visualization, and Integrated Discovery, Genome Biology, 4(9), http://genomebiology.com/2003/4/9/R60

Donaldson, K., Stone, V., Tran, C. L., Kreyling, W., & Borm, P. J. (2004). Nanotoxicology. Occupational and environmental medicine, 61(9), 727–728. doi:10.1136/oem.2004.013243

Edgar, R., & Barrett, T. (2006). NCBI GEO standards and services for microarray data. Nature biotechnology, 24(12), 1471–1472. doi:10.1038/nbt1206-1471

Galanzha, E. I., Weingold, R., Nedosekin, D. A., Sarimollaoglu, M., Nolan, J., Harrington, W., . . . Zharov, V. P. (2017). Spaser as a biological probe. Nat Commun, 8, 15528. doi:10.1038/ncomms15528

Guimaraes, R. S., Rodrigues, C. F., Moreira, A. F., & Correia, I. J. (2020). Overview of stimuli-responsive mesoporous organosilica nanocarriers for drug delivery. Pharmacol Res, 155, 104742. doi:10.1016/j.phrs.2020.104742

Jain, K. K. (2017). The handbook of nanomedicine. 3rd. Pages1-9 [electronic resource]. Humana Press. Retrieved from http://search.ebscohost.com/login.aspx?direct=true&db=cat00847a&AN=usflc.035093967&site=eds-live

James, N. D., Coker, R. J., Tomlinson, D., Harris, J. R. W., Gompels, M., Pinching, A. J., & Stewart, J. S. W. (1994). Liposomal doxorubicin (Doxil): An effective new treatment for Kaposi's sarcoma in AIDS. Clinical Oncology, 6(5), 294-296. doi:https://doi.org/10.1016/S0936-6555(05)80269-9

Jens-Uwe, A. H. J. R. H. M. (2008). Nanocrystal technology, drug delivery and clinical applications. International Journal of Nanomedicine, 2008(Issue 3), 295-309.

Lim, J. O., Shin, N. R., Seo, Y. S., Nam, H. H., Ko, J. W., Jung, T. Y., . . . Shin, I. S. (2020). Silibinin Attenuates Silica Dioxide Nanoparticles-Induced Inflammation by Suppressing TXNIP/MAPKs/AP-1 Signaling. Cells, 9(3). doi:10.3390/cells9030678

Juère, E., Caillard, R., Marko, D., Del Favero, G., & Kleitz, F. (2020). Smart Protein-Based Formulation of Dendritic Mesoporous Silica Nanoparticles: Toward Oral Delivery of Insulin. Chemistry - A European Journal, 26(23), 5195-5199. doi:10.1002/chem.202000773

Kiew, S. F., Kiew, L. V., Lee, H. B., Imae, T., & Chung, L. Y. (2016). Assessing biocompatibility of graphene oxide-based nanocarriers: A review. Journal of Controlled Release, 226, 217–228. doi: 10.1016/j.jconrel.2016.02.015

Kim, B. Y., Rutka, J. T., & Chan, W. C. (2010). Nanomedicine. New England Journal of Medicine, 363(25), 2434-2443. doi:10.1056/NEJMra0912273

Kohonen, P., Parkkinen, J. A., Willighagen, E. L., Ceder, R., Wennerberg, K., Kaski, S., & Grafstrom, R. C. (2017). A transcriptomics data-driven gene space accurately predicts liver cytopathology and drug-induced liver injury. Nat Commun, 8, 15932. doi:10.1038/ncomms15932

Kumar, A., Chen, F., Mozhi, A., Zhang, X., Zhao, Y., Xue, X., … Liang, X. J. (2013). Innovative pharmaceutical development based on unique properties of nanoscale delivery formulation. Nanoscale, 5(18), 8307–8325. doi:10.1039/c3nr01525d

Lai, J. C., Ananthakrishnan, G., Jandhyam, S., Dukhande, V. V., Bhushan, A., Gokhale, M., … Leung, S. W. (2010). Treatment of human astrocytoma U87 cells with silicon dioxide nanoparticles lowers their survival and alters their expression of mitochondrial and cell signaling proteins. International journal of nanomedicine, 5, 715–723. doi:10.2147/IJN.S5238

Li, J., Chang, X., Chen, X., Gu, Z., Zhao, F., Chai, Z., & Zhao, Y. (2014). Toxicity of inorganic nanomaterials in biomedical imaging. Biotechnology Advances, 32(4), 727–743. doi: 10.1016/j.biotechadv.2013.12.00

Li, Z., Xu, J., Cui, H., Song, J., Chen, J., & Wei, J. (2020). Bioinformatics analysis of key biomarkers and potential molecular mechanisms in hepatocellular carcinoma induced by hepatitis B virus. Medicine (Baltimore), 99(20), e20302. doi:10.1097/MD.0000000000020302

Liao, K.-H., Lin, Y.-S., Macosko, C. W., & Haynes, C. L. (2011). Cytotoxicity of Graphene Oxide and Graphene in Human Erythrocytes and Skin Fibroblasts. ACS Applied Materials & Interfaces, 3(7), 2607–2615. doi: 10.1021/am200428v

Lovett, R. A. (2000). Toxicogenomics. Toxicologists brace for genomics revolution. Science, 289(5479), 536-537. doi:10.1126/science.289.5479.536

Moos, P. J., Honeggar, M., Malugin, A., Herd, H., Thiagarajan, G., & Ghandehari, H. (2013). Transcriptional responses of human aortic endothelial cells to nanoconstructs used in biomedical applications. Molecular pharmaceutics, 10(8), 3242–3252. doi:10.1021/mp400285u

Nafisi, S., & Maibach, H. I. (2015). Silica Nanoparticles for Increased Cosmetic Ingredient Efficacy. Cosmetics & Toiletries, 130(4), 36-43.

Nawroth, P., & Stern, D. (1987). Tumor Necrosis Factor/Cachectin-Induced Modulation of Endothelial Cell Hemostatic Properties. Oncology Research and Treatment, 10(4), 254–258. doi: 10.1159/000216415

Oberdörster, G., Oberdörster, E., & Oberdörster, J. (2005). Nanotoxicology: an emerging discipline evolving from studies of ultrafine particles. Environmental health perspectives, 113(7), 823–839. doi:10.1289/ehp.7339

Okada, Y., Kato, M., Minakami, H., Inoue, Y., Morikawa, A., Otsuki, K., & Kimura, H. (2001). REDUCED EXPRESSION OF FLICE-INHIBITORY PROTEIN (FLIP) AND NFκB IS ASSOCIATED WITH DEATH RECEPTOR-INDUCED CELL DEATH IN HUMAN AORTIC ENDOTHELIAL CELLS (HAECs). Cytokine, 15(2), 66–74. doi: 10.1006/cyto.2001.0916

Old, Lloyd J. (1985). Tumor necrosis factor. Science, 230, 1 p. 630. https://link.gale.com/apps/doc/A4015538/AONE?u=tamp44898&sid=AONE&xid=1d9ab150. Accessed 22 Jan. 2020.

Patil, L. D., Verma, U., Patil, U. D., Naik, J. B., & Narkhede, J. S. (2019). Inclusion of Aceclofenac in Mesoporous Silica Nanoparticles: Drug Release Study and Statistical Optimization of Encapsulation Efficiency by Response Surface Methodology. Materials Technology, 34(12), 751-763. doi:10.1080/10667857.2019.1624301

Patra, J. K., Das, G., Fraceto, L. F., Campos, E. V. R., Rodriguez-Torres, M. D. P., Acosta-Torres, L. S., . . . Shin, H. S. (2018). Nano based drug delivery systems: recent developments and future prospects. J Nanobiotechnology, 16(1), 71. doi:10.1186/s12951-018-0392-8

Pirutchada, M., Marie, B. S., Iseult, L., Siriwat, S., N, C., & Eugenia, V.-J. (2019). Silica Nanoparticle Synthesis and Multi-Method Characterisation. Materials Science Forum, 947, 82-90. doi:10.4028/www.scientific.net/MSF.947.82

Skuland, T., Lag, M., Gutleb, A. C., Brinchmann, B. C., Serchi, T., Ovrevik, J., . . . Refsnes, M. (2020). Pro-inflammatory effects of crystalline- and nano-sized non-crystalline silica particles in a 3D alveolar model. Part Fibre Toxicol, 17(1), 13. doi:10.1186/s12989-020-00345-3

Tilton, S. C., Karin, N. J., Tolic, A., Xie, Y., Lai, X., Hamilton, R. F., … Orr, G. (2013). Three human cell types respond to multi-walled carbon nanotubes and titanium dioxide nanobelts with cell-specific transcriptomic and proteomic expression patterns. Nanotoxicology, 8(5), 533–548. doi: 10.3109/17435390.2013.803624

Wang, M., Wang, T., Wang, D., Jiang, W., & Fu, J. (2019). Acid and light stimuli-responsive mesoporous silica nanoparticles for controlled release. Journal of Materials Science, 54(8), 6199-6211. doi:10.1007/s10853-019-03325-x

Weinberg, J. M., & Buchholz, R. (2006). TNF-alpha inhibitors. [electronic resource]: Birkhäuser Verlag.

Wilhelm, S., Tavares, A. J., Dai, Q., Ohta, S., Audet, J., Dvorak, H. F., & Chan, W. C. W. (2016). Analysis of nanoparticle delivery to tumours. Nature Reviews Materials, 1(5). doi: 10.1038/natrevmats.2016.14 P.1-12

Yan M, Zhang Y, Xu KD, Fu T, Qin HY, Zheng XX. An in vitro study of vascular endothelial toxicity of CdTe quantum dots. Toxicology 2011;282(3):94–103.

Yang, Y., Zhao, W., Tan, W., Lai, Z., Fang, D., Jiang, L., . . . Lai, Y. (2019). An Efficient Cell-Targeting Drug Delivery System Based on Aptamer-Modified Mesoporous Silica Nanoparticles. Nanoscale Research Letters, 14(1), 1-10. doi:10.1186/s11671-019-3208-3

Zhu MT, Wang B, Wang Y, Yuan L, Wang HJ, Wang M, et al. Endothelial dysfunction and inflammation induced by iron oxide nanoparticle exposure: risk factors for early atherosclerosis. Toxicol Lett (2011);203:162–7.

Zhu MT, Wang Y, Feng WY, Wang B, Wang M, Ouyang H, et al. Oxidative stress and apoptosis induced by iron oxide nanoparticles in cultured human umbilical endothelial cells. J Nanosci Nanotechnol (2010);10:8584–90.

Appendix

Abbreviation list

COOH: carboxyl

DAVID: Database for Annotation, Visualization and Integrated Discovery

GEO: Gene Expression Omnibus

HAECs: human aortic endothelial cells

HBV: hepatitis B virus

HCC: hepatocellular carcinoma

MSNPs: mesoporous silica nanoparticles

NCBI: National Center for Biotechnology Information

NH_2: amine

NPs: nanoparticles

PAMAM: poly-amido-amine

SiO_2: silicon dioxide

SNPs: silica nanoparticles

TiO_2: titanium dioxide

TiO_2-NB: nanobelts

TNF: tumor necrosis factor

UV: ultraviolet